DØ Note 6297-CONF

Search for a Fermiophobic Higgs Boson in the di-photon final state using 9.7 fb^{-1} of DØ data

The DØ Collaboration
URL http://www-d0.fnal.gov
(Dated: February 28, 2012)

This note describes a search for a Fermiophobic Higgs boson (h_f) in the di-photon final state using DØ data corresponding to an integrated luminosity of 9.7 fb^{-1}, collected at the Fermilab Tevatron collider from April 2002 to September 2011. We set 95% C.L. upper limits on the cross section times the branching ratio ($\sigma \times BR(h_f \to \gamma\gamma)$) and the branching ratio ($BR(h_f \to \gamma\gamma)$) for different assumed Higgs masses from 100 GeV to 150 GeV. The sensitivity reaches 114 GeV, well beyond that of the combined LEP experiments. We exclude Fermiophobic Higgs particles with a mass $M_{h_f} < 111.4$ GeV.

Preliminary Results for Winter 2012 Conferences

I. INTRODUCTION

A search for standard model (SM) Higgs bosons in the $H \to \gamma\gamma$ channel is challenging due to its small branching ratio of this process. For instance, it is $\sim 0.22\%$ for a Higgs boson with a mass of 120 GeV. However, the branching ratio is enhanced significantly in some models beyond the SM [1]. In the model of Fermiophobic Higgs bosons (h_f), which assumes zero coupling of the Higgs boson to fermions, the branching ratio is enhanced by about an order of magnitude (see Table I). This hypothesis has been searched for at LEP [2], the Tevatron [3] and the LHC [4]. The gluon-gluon fusion Higgs Boson production mechanism, which is dominant at the Tevatron, involves a top quark loop and so is suppressed in the Fermiophobic Higgs model. Therefore, the main production mechanisms are associate vector boson ($h_f + V \to \gamma\gamma + V$, $V = W, Z$) and vector boson fusion (VBF $h_f \to \gamma\gamma$) in this model. The coupling strength of a Fermiophobic Higgs boson to V is assumed to be the same as that of a SM Higgs boson.

In this analysis, we use data corresponding to 9.7 fb^{-1} of DØ Run II data and utilize the same analysis technique as Ref [5]. A Multivariate Analysis Technique (MVA) [6] is used to combine ten kinematic variables to build a final discriminant between signal and background to enhance the sensitivity.

m_{h_f} (GeV)	100	110	120	130	140	150
$BR(H \to \gamma\gamma)$	0.0015	0.0019	0.0022	0.0022	0.0019	0.0014
$BR(h_f \to \gamma\gamma)$	0.185	0.060	0.023	0.011	0.005	0.0030
$BR(h_f \to \gamma\gamma)/BR(H \to \gamma\gamma)$	123	32	10	5	3	2

TABLE I: Branching Ratio comparison for a SM Higgs boson and a Fermiophobic Higgs boson into two photons. $BR(H \to \gamma\gamma)$ and $BR(h_f \to \gamma\gamma)$ stand for the branching ratios of a SM Higgs boson and a Fermiophobic boson into two photons respectively.

The DØ detector, the data samples, event selection, background estimation and modeling and the associated systematic uncertainties (except those for gluon-gluon fusion process) are the same as described in the search for the SM Higgs boson (Ref. [5]). Below we describe only what is specific to this analysis, namely the signal simulation, separation of the signal from the SM background and limit setting.

II. SIGNAL SIMULATION

Since only gluon-gluon fusion process is absent, we use the same VH and VBF signal samples that are normalized to the same SM cross sections as [5]. However, the branching ratios for each mass point are different from those in SM, and are obtained from HDECAY [7] calculations specifically for Fermiophobic Higgs bosons.

III. FINAL DISCRIMINANT DISTRIBUTIONS AND LIMITS

A. Final discriminant distributions

To improve the overall sensitivity, we use the gradient Boosted Decision Tree method (BDTG) from the Toolkit for Multivariate Analysis [6] that combines ten kinematic variables to build a final discriminant between the signal and background. The ten kinematic variables we used are,

- leading photon transverse momentum, p_T^1;
- sub-leading photon transverse momentum, p_T^2
- di-photon invariant mass, $M_{\gamma\gamma}$;
- di-photon transverse momentum, $p_T^{\gamma\gamma}$;
- azimuthal angle between the two photon candidates, $\Delta\phi_{\gamma\gamma}$.
- $\cos\theta^*$, in Collins-Soper frame [8];
- ϕ^*, in Collins-Soper frame;
- leading photon ANN output, ONN^1;
- sub-leading photon ANN output, ONN^2;

- missing transverse energy $\not{E}_T$.

Figures 1 and 2 show these ten kinematic distributions from data, backgrounds and the $M_{h_f} = 115$ GeV signal. The signal and total background samples are trained for every mass point displayed in Table II using events within a [M_{h_f} - 30GeV, M_{h_f} + 30GeV] mass window. At the 2.5 GeV mass points we interpolate the MVA input from the neighbouring 5 GeV points using the fact that the selection efficiency is almost independent of the di-photon mass and the mass resolution is approximately constant (~ 3 GeV). As an illustration, we show the MVA output distributions for six of the hypothetic Fermiophobic Higgs masses in Fig. 3.

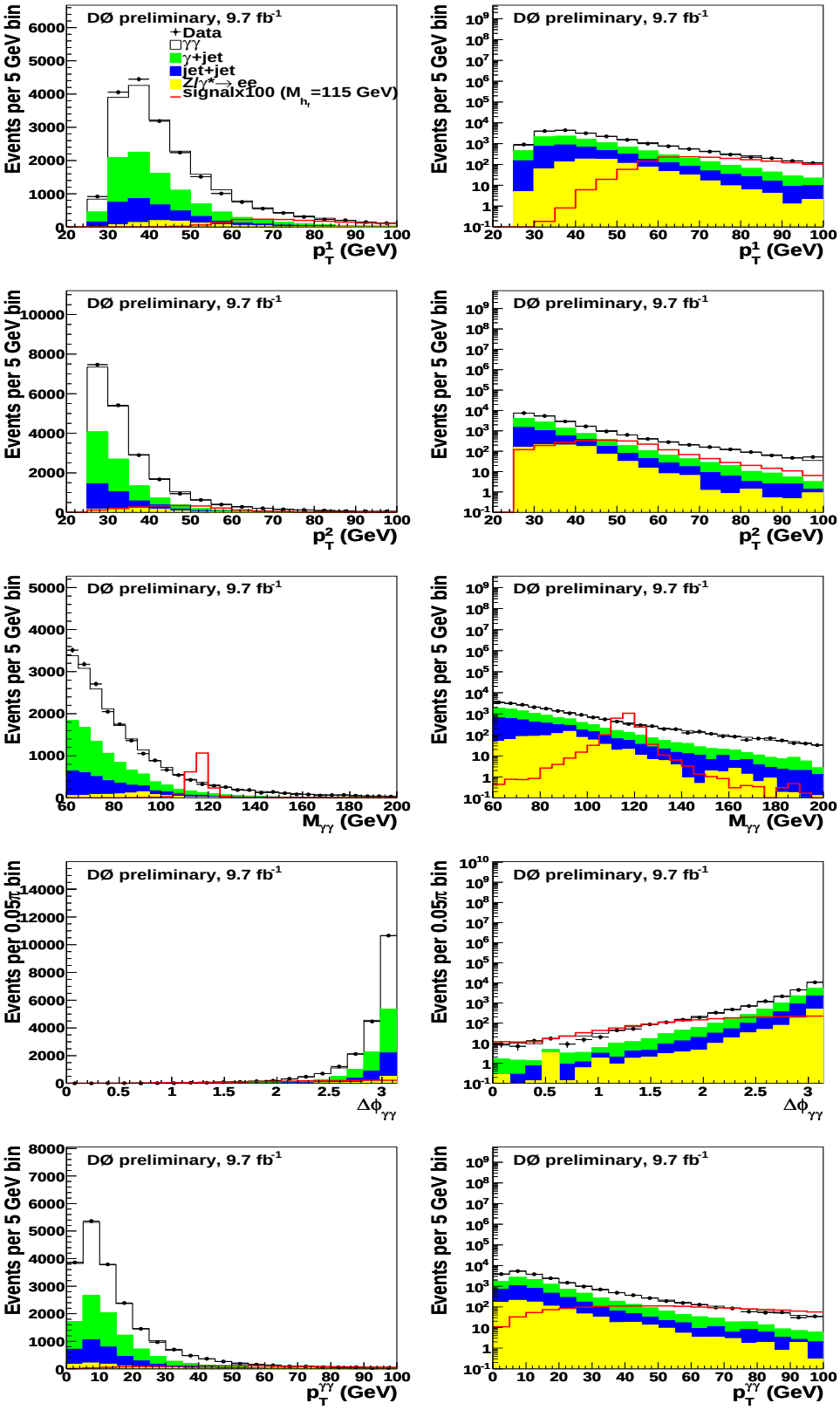

FIG. 1: Data and background modeling comparisons in terms of p_T^1, p_T^2, $M_{\gamma\gamma}$, $\Delta\phi^{\gamma\gamma}$ and $p_T^{\gamma\gamma}$ for the mass region [60, 200] GeV. A signal for $M_{h_f} = 115$ GeV, multiplied by 100 is also shown. The plots in the left column are in linear scale and the plots in the right column are in log scale. The legend is shown in top left plot.

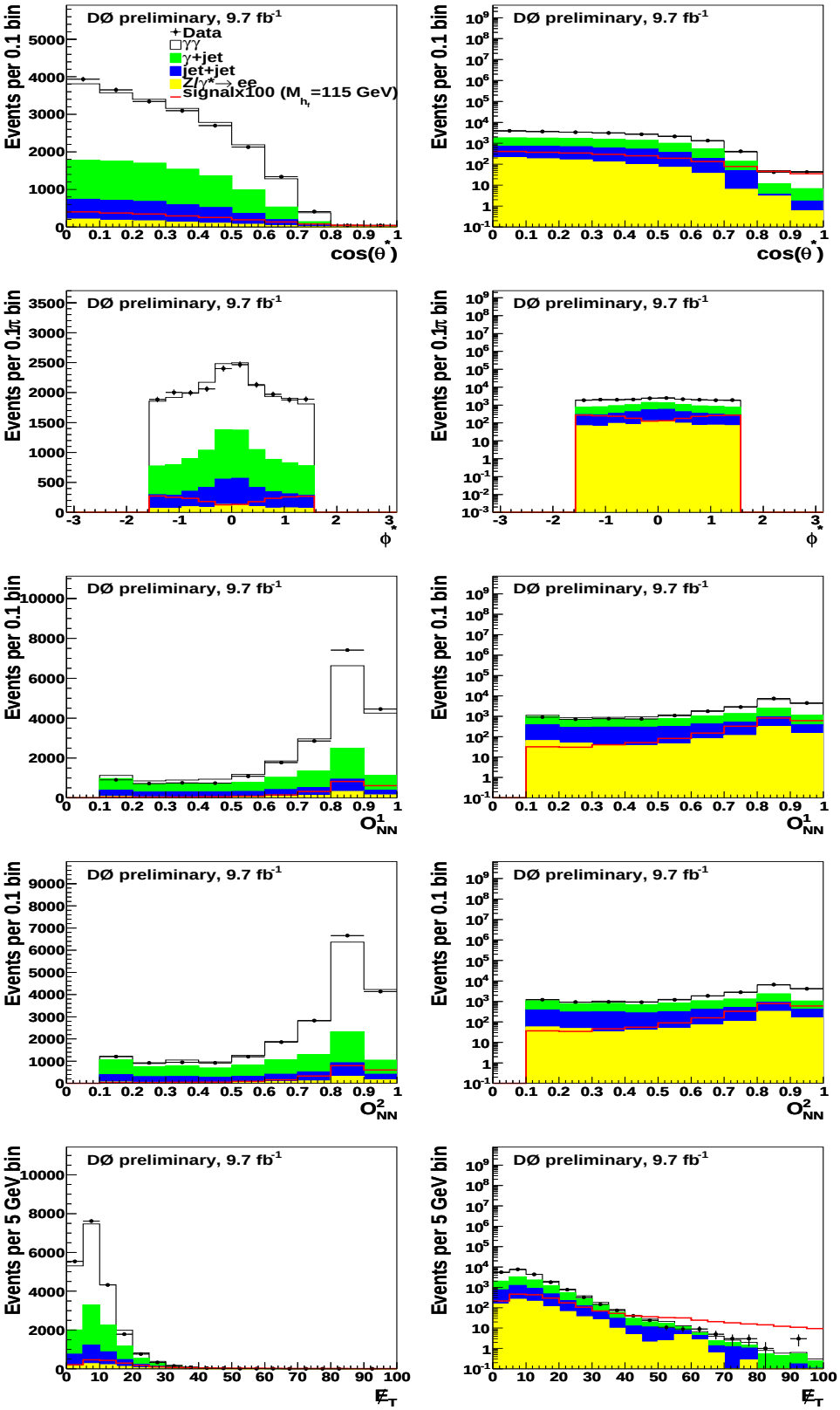

FIG. 2: Data and background modeling comparisons in terms of $\cos\theta^*$, ϕ^*, ONN^1, ONN^2 and $\not\!\!E_T$ for the mass region [60, 200] GeV. A signal for $M_{h_f} = 115$ GeV, multiplied by 100 is also shown. The plots in the left column are in linear scale and the plots in the right column are in log scale. The legend is the same as Fig. 1.

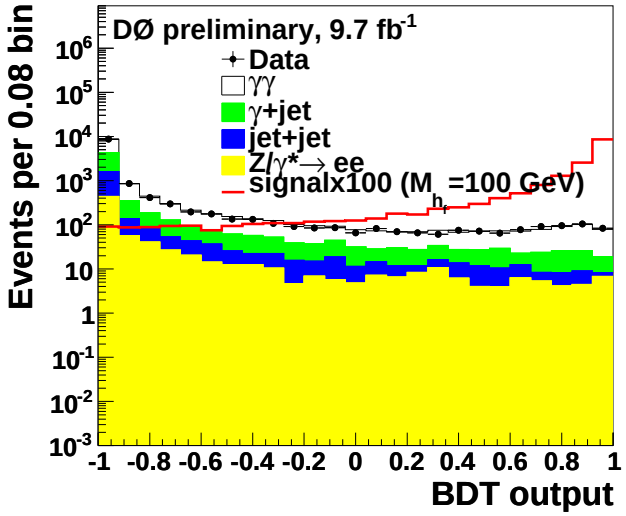

(a)$M_{h_f} = 100$ GeV

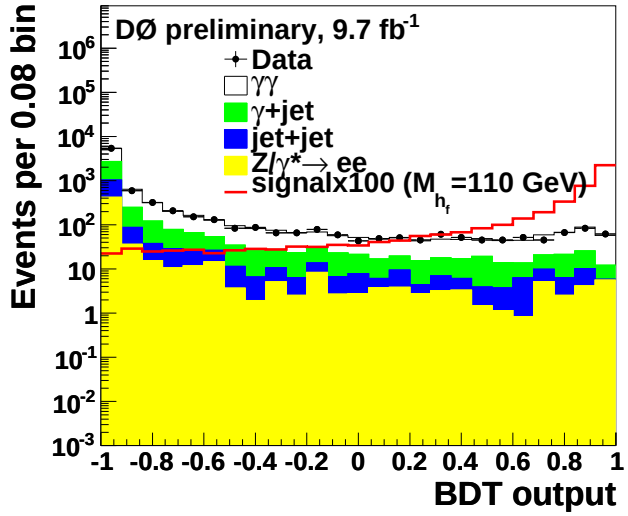

(b)$M_{h_f} = 110$ GeV

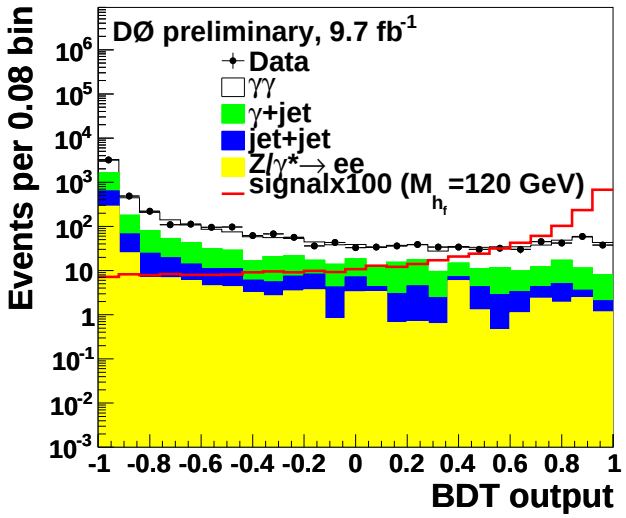

(c)$M_{h_f} = 120$ GeV

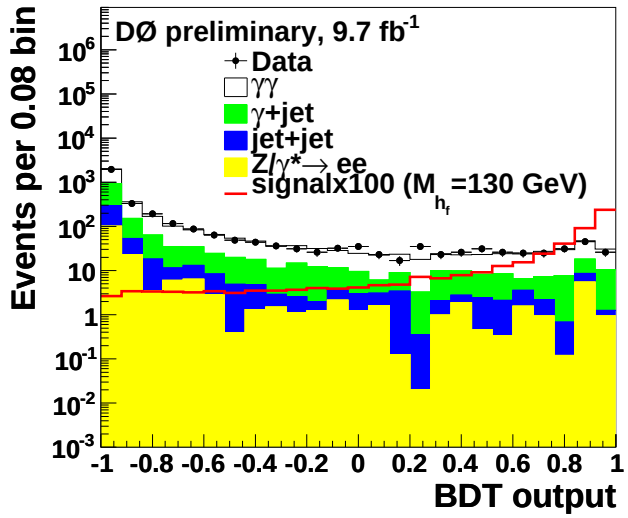

(d)$M_{h_f} = 130$ GeV

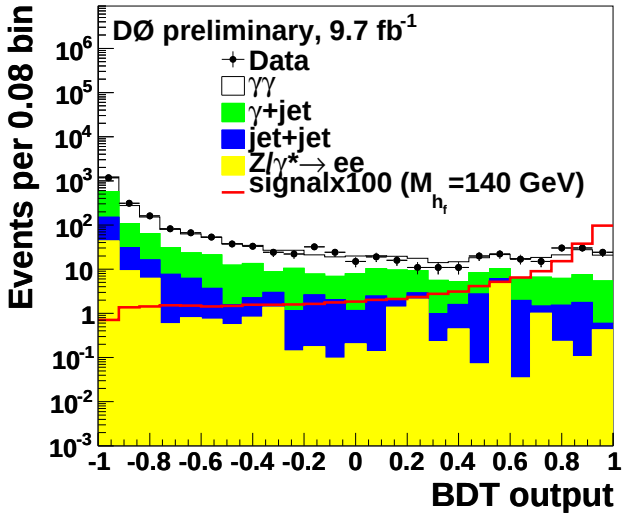

(e)$M_{h_f} = 140$ GeV

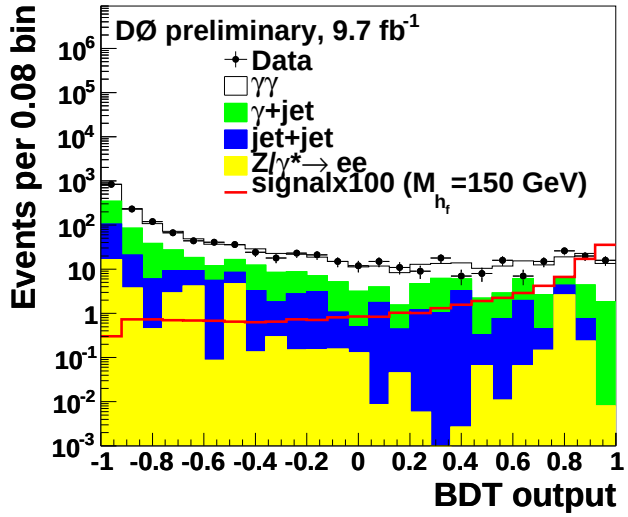

(f)$M_{h_f} = 150$ GeV

FIG. 3: MVA output distributions for $M_{h_f} = 100 - 150$ GeV in 10 GeV intervals. Each mass point has a mass window selection of ± 30 GeV.

Higgs mass(GeV)	100	102.5	105	107.5	110	112.5	115	117.5	120	122.5
observed limit(fb)	27.1	25.3	23.3	22.3	19.7	21.3	14.8	13.1	9.1	9.7
expected limit(fb)	21.3	20.5	19.6	16.9	15.7	14.7	14.4	14.2	12.9	12.9

Higgs mass(GeV)	125	127.5	130	132.5	135	137.5	140	142.5	145	147.5	150
observed limit(fb)	10.0	9.2	10.6	11.5	12.7	12.7	11.6	12.0	10.1	10.3	8.7
expected limit(fb)	13.4	13.0	12.5	12.2	10.9	9.8	9.4	9.6	9.0	8.8	8.4

TABLE II: 95% C.L. observed and expected limits on $\sigma \times BR(h_f \to \gamma\gamma)$ for different Fermiophobic Higgs masses.

B. Limit setting

We set upper limits on the cross section times branching ratio and the branching ratio for a Fermiophobic Higgs boson decaying into a pair of photons, using the MVA output distributions for each mass point in the interval of [M_{h_f} - 30 GeV, M_{h_f} + 30 GeV]. The limits are calculated at the 95% confidence level using the modified frequentist CL_S approach with a Poisson log-likelihood ratio test statistic [9]. Systematic uncertainties are treated as nuisance parameters constrained by their priors, and the best fits of these parameters to data are determined at each value of M_{h_f} by maximizing the likelihood ratio [10]. The correlations of the systematic uncertainties are maintained.

As an illustration, the background subtracted data distribution at 115 GeV is shown in Fig. 4.

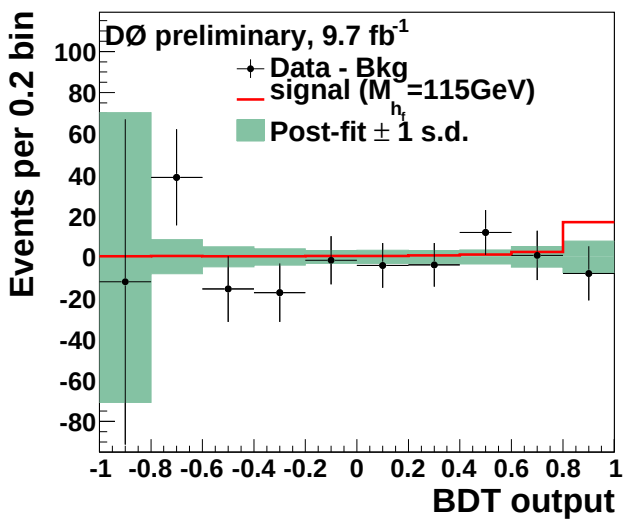

FIG. 4: Post-fit background subtracted data distribution for M_{h_f} = 115 GeV. The green area shows the post-fit 1 standard deviation (s.d.) under S+B hypothesis and nominal signal yields are considered.

Table II and Fig. 5(left) show the upper limits on $\sigma \times BR(h_f \to \gamma\gamma)$ for the different hypothetic Fermiophobic Higgs masses. By assuming the SM cross section for the associated vector boson and vector boson fusion Higgs production mechanism, we also derive the upper limits on the $BR(h_f \to \gamma\gamma)$ as a function of the Fermiophobic Higgs mass (see Table III and Fig. 5(right)).

IV. SUMMARY

We have presented a search for Fermiophobic Higgs bosons in the di-photon channel using 9.7 fb^{-1} DØ Run II data. We set 95% C.L. upper limits on the $\sigma \times BR(h_f \to \gamma\gamma)$ and $BR(h_f \to \gamma\gamma)$ for hypothetic Fermiophobic Higgs masses. The expected exclusion reaches 114 GeV, well beyond that of the combined LEP experiments. We exclude Fermiophobic Higgs particles with a mass of $M_{h_f} < 111.4$ GeV.

Higgs mass(GeV)	100	102.5	105	107.5	110	112.5	115	117.5	120	122.5
observed limit(%)	6.2	4.8	5.5	5.3	5.0	5.5	4.3	3.5	3.7	3.2
expected limit(%)	4.0	4.1	4.3	3.9	4.0	3.8	4.3	4.3	4.7	4.8
theory $BR(h_f \to \gamma\gamma)$ (%)	18.5	13.9	10.4	7.9	6.0	4.7	3.7	2.9	2.3	1.9

Higgs mass(GeV)	125	127.5	130	132.5	135	137.5	140	142.5	145	147.5	150
observed limit(%)	2.6	4.0	4.3	6.1	7.6	6.1	7.4	6.3	8.3	7.6	7.2
expected limit(%)	5.1	5.2	5.4	4.9	5.0	5.1	5.3	5.5	5.8	5.5	5.8
theory $BR(h_f \to \gamma\gamma)$ (%)	1.6	1.3	1.1	0.9	0.8	0.6	0.5	0.5	0.4	0.3	0.3

TABLE III: 95% C.L. observed and expected limits on $BR(h_f \to \gamma\gamma)$ for different Fermiophobic Higgs masses. Also shown are the theory predictions.

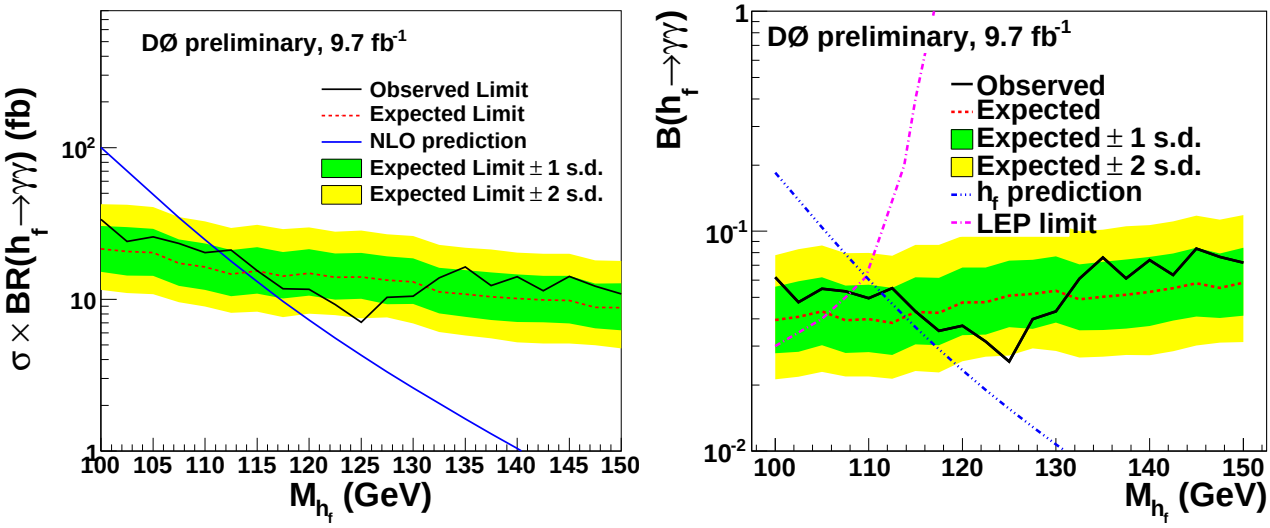

FIG. 5: 95% C.L. upper limits on $\sigma \times BR$ (left) and BR (right) as a function of Fermiophobic Higgs masses. The observed limit is shown as a solid black line while the expected limit under the background-only hypothesis is shown as a dashed red line. The green and yellow areas correspond to the 1 and 2 standard deviations (s.d.) around the expected limit.

Acknowledgments

We thank the staffs at Fermilab and collaborating institutions, and acknowledge support from the DOE and NSF (USA); CEA and CNRS/IN2P3 (France); FASI, Rosatom and RFBR (Russia); CAPES, CNPq, FAPERJ, FAPESP and FUNDUNESP (Brazil); DAE and DST (India); Colciencias (Colombia); CONACyT (Mexico); KRF and KOSEF (Korea); CONICET and UBACyT (Argentina); FOM (The Netherlands); STFC (United Kingdom); MSMT and GACR (Czech Republic); CRC Program, CFI, NSERC and WestGrid Project (Canada); BMBF and DFG (Germany); SFI (Ireland); The Swedish Research Council (Sweden); CAS and CNSF (China); and the Alexander von Humboldt Foundation.

[1] S. Mrenna and J. Wells, Phys. Rev. D **63**, 015006 (2000).

[2] A. Heister *et al.* (ALEPH Collaboration), Phys. Lett. B **544**, 16 (2002);
P. Abreu *et al.* (DELPHI Collaboration), Phys. Lett. B **507**, 89 (2001); Eur. Phys. J. C **35**, 313, (2004);
G. Abbiendi *et al.* (OPAL Collaboration), Phys. Lett. B **544**, 44 (2002);
P. Achard *et al.* (L3 Collaboration), Phys. Lett. B **534**, 28 (2002); Phys. Lett. B **568**, 191 (2003);
LEP (LEP Higgs Working Group) arXiv:hep-ex/0107035 (2001).

[3] B. Abbott *et al.* (DØ Collaboration), Phys. Rev. Lett. **82**, 2244 (1999);
T. Affolder *et al.* (CDF Collaboration), Phys. Rev. D **64**, 092002 (2001);

V.M. Abazov *et al.* (DØ Collaboration), Phys. Rev. Lett. **101**, 051801 (2008).
[4] CMS Collaboration, CMS-HIG-11-021, (2011);
ATLAS Collaboration, ATLAS-CONF-2011-149, (2011).
[5] DØ Collaboration, DØ Note **6295-CONF** (2012). http://www-d0.fnal.gov/Run2Physics/WWW/documents/Run2Results.htm
[6] A. Hoecker *et al.*, TMVA 4 Toolkit for Multivariate Data Analysis with ROOT Users Guide, arXiv:physics/0703039 (2007).
[7] A. Djouadi, J. Kalinowski and M. Spira, Comput. Phys. Commun. **108**, 56 (1998).
[8] J.C. Collins and D.E. Soper, Phys. Rev. D **16**, 2219 (1977).
[9] T. Junk, Nucl. Intrum. Methods A **434**, 435 (1999); A. Read, CERN 2000-005 (2000).
[10] W. Fisher, FERMILAB-TM-2386-E (2006).